substance: LaH_x
property: crystal structure, physical properties

crystal structure		cubic (O_h^5 – Fm3m)		55M, 57S, 59S
semiconductor: x = 2.7		T < 239 K		79B, 79Z
semiconductor: x = 3.0		T < 241 K		83I
energy gap				
E_g	0.1 eV	T < 210 K		80B
Debye temperature				
Θ_D	241.5 K	x = 3		83I

LaH_{2+x} [95V]

			phase diagram: Fig. 2	
semiconductor:	x = 0.70		M-SC transition: T = 260(10) K (heating)	88S,
ρ	850 μΩcm	T = 260 K		90S
semiconductor:	x = 0.80		M-SC transition: T = 230(10) K (heating)	88S,
ρ	5000 μΩcm	T = 230 K		90S
semiconductor:	x = 0.84		M-SC transition: T = 220(5) K (heating)	88S,
ρ	$3 \cdot 10^4$ μΩcm	T = 220 K		90S
semiconductor:	x = 0.90		M-SC transition: T = 260(3) K (heating)	88S,
ρ	$6 \cdot 10^5$ μΩcm	T = 260 K		90S
			normalized resistivity vs. T: Fig. 4,	
			XPS-spectrum: Fig. 1, UPS-spectrum: Fig. 3	

Further figures and references:

crystal structure: Fig. 5

lattice parameter vs. x: Fig. 6

heat capacity [79B, 83I] and **semiconductor-metal transition**: Fig. 7 (x = 3) and Fig. 8 (x = 2.7)

band structure (x = 3): Figs. 9, 10

density-of-states (x = 3): Figs. 10, 11

proposed electronic level scheme (x = 3): Fig. 12

temperature dependence of **electrical resistivity** (x = 2.85): Fig. 13

XPS spectra (x = 3): Figs. 14, 15

EDC spectra (x = 2.89): Figs. 16, 17

hydrogen vibrations [82 K]

optical phonon energies of 116 meV and 64 meV for x = 2.82 [71M]

References:

53Z Ziegler, W. T., Young, R. A.: Phys. Rev. 90 (1953) 115.

55H Holley, C. E., Mulford, R. N. R., Ellinger, F. H., Koehler, W. C., Zachariasen, W. H.: J. Phys. Chem. 59 (1955) 1226.

55M Mulford, R. N. R., Holley, C. E., Jr.: J. Phys. Chem. 59 (1955) 1222.

55S Stalinski, B.: Bull. Acad. Pol. Sci., C1 III, 3 (1955) 613.

57S Stalinski, B.: Bull. Acad. Pol. Sci. 5 (1957) 1001.

59G Goon, E. J.: J. Phys. Chem. 63 (1959) 2018.

59S Stalinski, B.: Bull. Acad. Pol., Sci., 7 (1959) 269.

66K Korst, W. L., Warf, J. C.: Inorg. Chem. 5 (1966) 1719.

66M Messer, C. E., Miller, R. M., Barrante, J. R.: Inorg. Chem. 5 (1966) 1814.

71M Macland, A. J., Holmes, D. E.: J. Chem. Phys. 54 (1971) 3979.

79B Bieganski, Z., Stalinski, B.: Z. Phys. Chem. Neue Folge 116 (1979) 109.

79M Müller, H., Knappe, P., Greis, O.: Z. Phys. Chem. 114 (1979) 45.

79Z Zogal, O. J.: Phys. Status Solidi (a) 53 (1979) K203.

80B Barnes, R. G., Beaudry, B. J., Creel, R. B., Torgeson, D. R., de Groot, D. G.: Solid State Commun. 36 (1980) 105.

80G Gupta, M., Burger, J. P.: Phys. Rev. B 22 (1980) 6074.

81P Peterman, D. J., Weaver, J. H., Peterson, D. T.: Phys. Rev. B23 (1981) 3903.

82M Misemer, D. K., Harmon, B. N.: Phys. Rev. B 26 (1982) 5634.

82S Schlapbach, L., Scherrer, H. R.: Solid State Commun. 41 (1982) 893.

83I Ito, T., Beaudry, B. J., Gschneidner, K. A., Takeshita, T.: Phys. Rev. B 27 (1953) 2830.

85O Osterwalder, J: Z. Phys. B 61 (1985) 113.

87S Schlapbach, L., Burger, J.P., Bonnet, J.E., Thiry, P., Petroff, Y.: Surf. Sci. 189/190 (1987) 747.

88S Shinar, J., Dehner, B., Beaudry, B.J., Peterson, D.T.: Phys. Rev. B 37 (1988) 2066.

89B Boroch, E., Kaldis, E.: Z. Phys. Chem. NF 163 (1989) 117;.

90S Shinar, J., Dehner, B., Barnes, R.G., Beaudry, B.J.: Phys. Rev. Lett. 64 (1990) 563.

95V Vajda, P.: "Hydrogen in rare-earth metals, including RH_{2+x} Phases" in: Handbook on the Physics and Chemistry of Rare Earth, Vol. 20, Gschneidner, K.A., Jr., Eyring, L. (eds.), Elsevier Science, 1995, p. 207.

Fig. 1.

RH_x. Valence band spectra for La, Y, Ce, and Pr and for their phase boundary and trihydride compositions from XPS. Data for the metals are shown by dotted lines [85O].

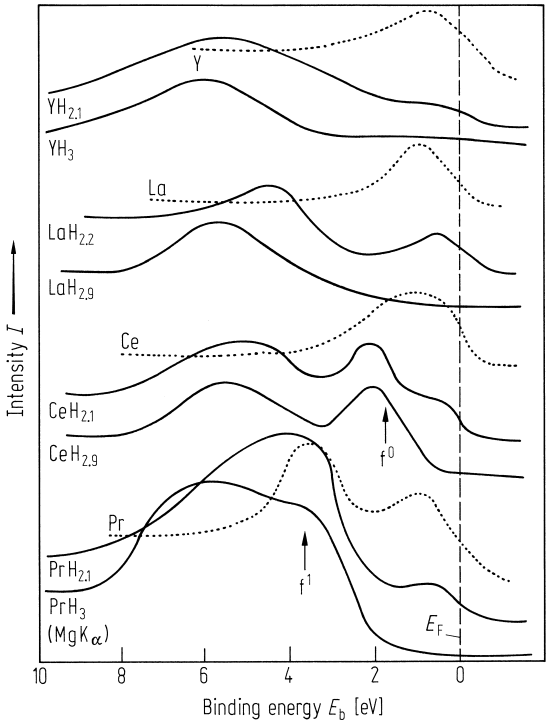

Fig. 2.

LaH_x. Representative phase diagram for the early-lanthanide hydride systems based on X-ray diffraction data for La + H [89B].

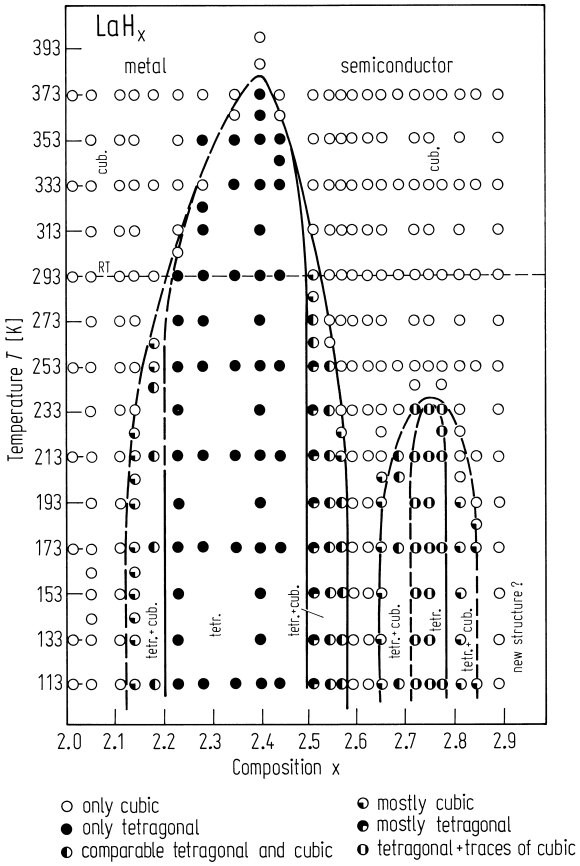

Fig. 3.

RH_x. UPS photoemission data for hydrides of La, Ce, Gd, and Tb at binding energies near the Fermi level [87S].

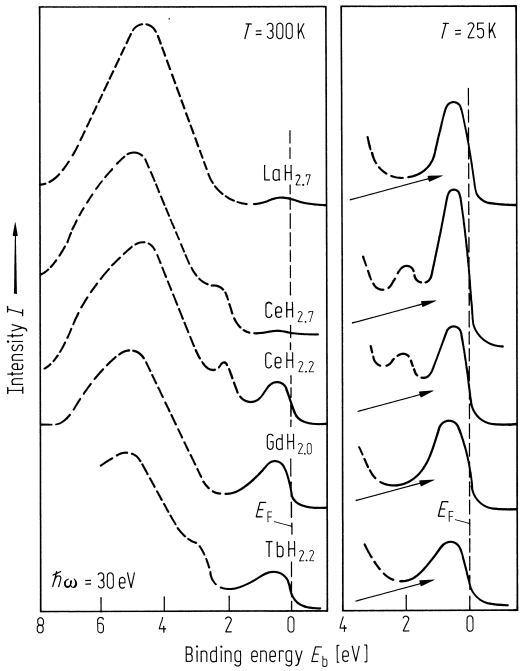

Fig. 4.

LaH_x. Normalized resistivity $\rho(T)/\rho(295K)$ as a function of the (inverse) temperature, showing the metal-semiconductor transition [90S].

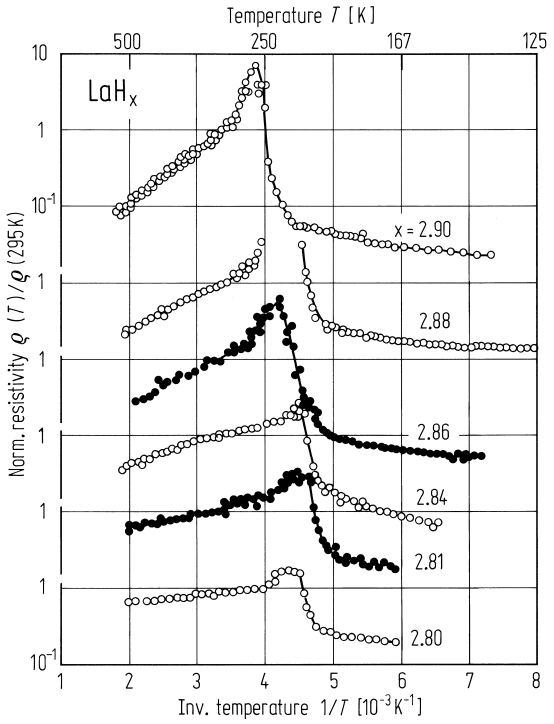

Fig. 5.

REH_x. Unit cell of the CaF_2-type structure.

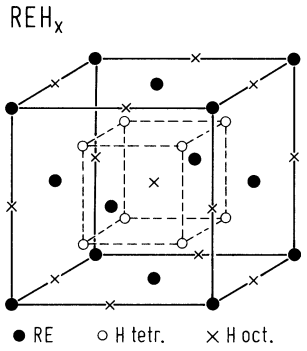

Fig. 6.

LaH_x, LaD_x. Lattice parameters of LaH_x (a) and LaD_x (b) as a function of x. For comparison the data of previous works are also shown [79M]. Data from [53Z, 55H, 55S, 59G, 66K, 66M, 79M].

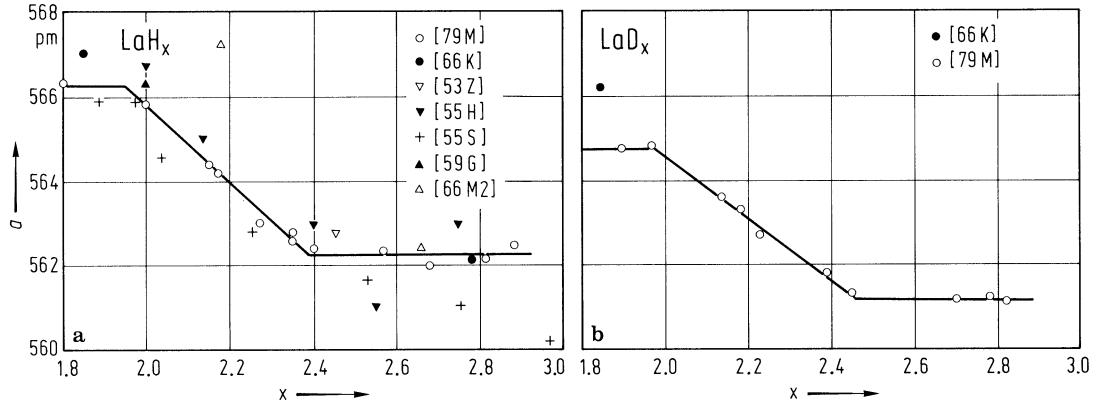

Fig. 7.

LaH_3, LaD_3. Temperature dependence of heat capacities. I, II, III and IV denote phase transitions. α: semiconductor; β: metal; γ, δ, ε: phases with different H- and D-distribution on lattice sites [83I].

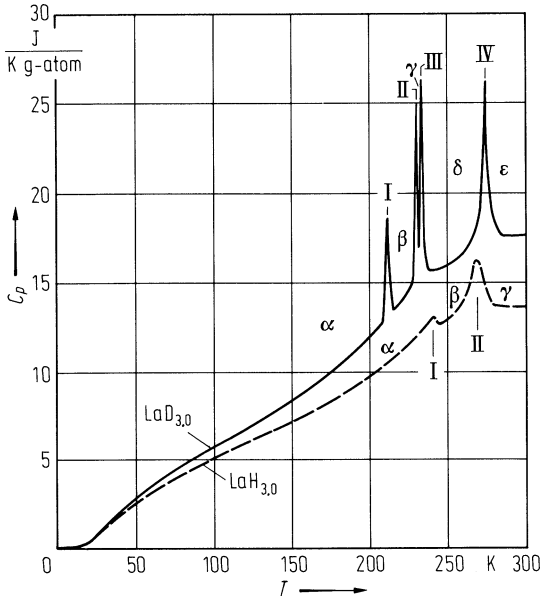

Fig. 8.

RH_x, R = La, Ce, Pr, Nd, Sm. Molar heat capacities vs. temperature. The maxima at about 250 K are attributed to metal-semiconductor transitions. No anomaly was found for $CeH_{2.96}$ and $SmH_{2.84}$ in this temperature range [79B].

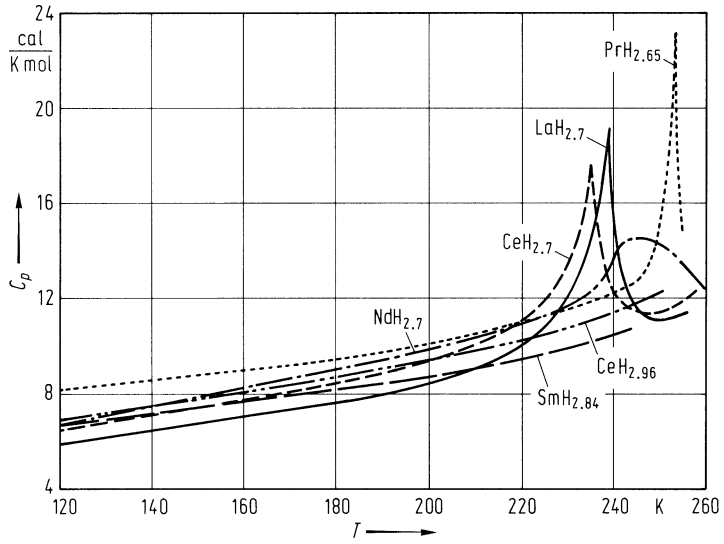

Fig. 9.

LaH_3. Energy bands of LaH_3 along several high-symmetry directions. Energies are in Rydberg [80G].

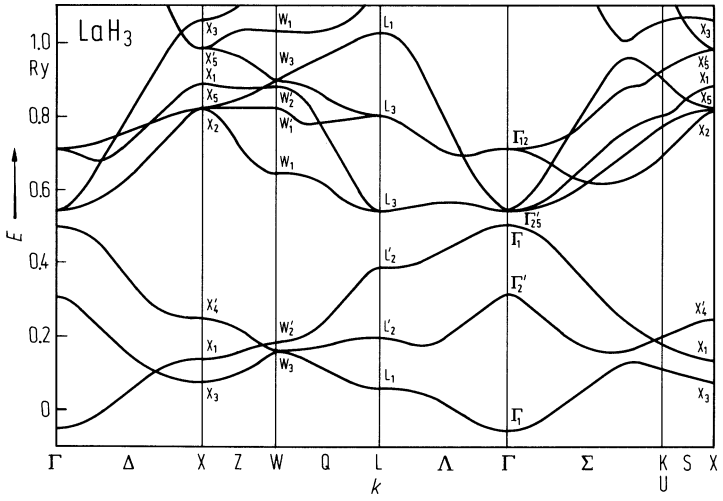

Fig. 10.

LaH_3. Energy bands and density of states [82M].

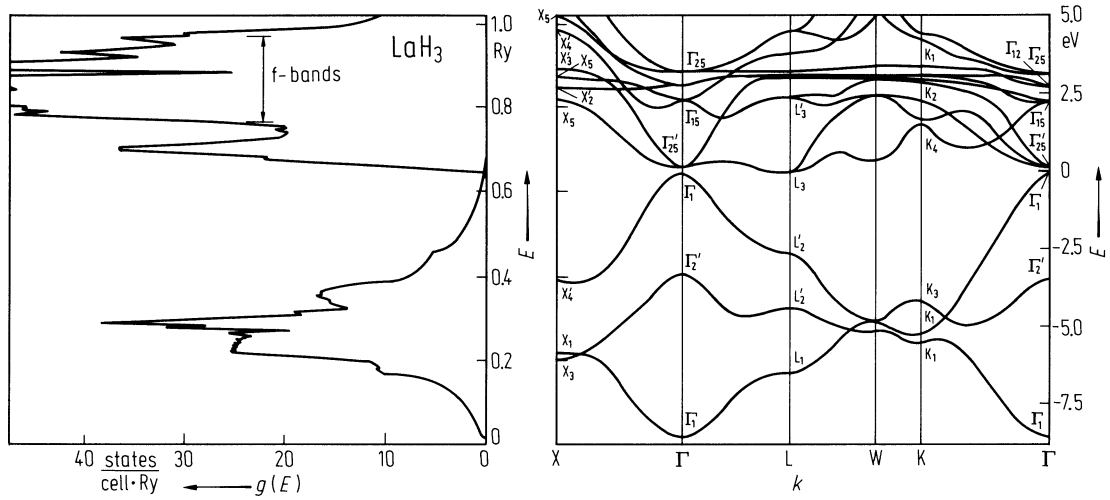

Fig. 11.

LaH_3. Density of states (solid curve) and number of electrons (dashed curve). Unit for $g(E)$ is states of both spins per Ry·unit cell [80G].

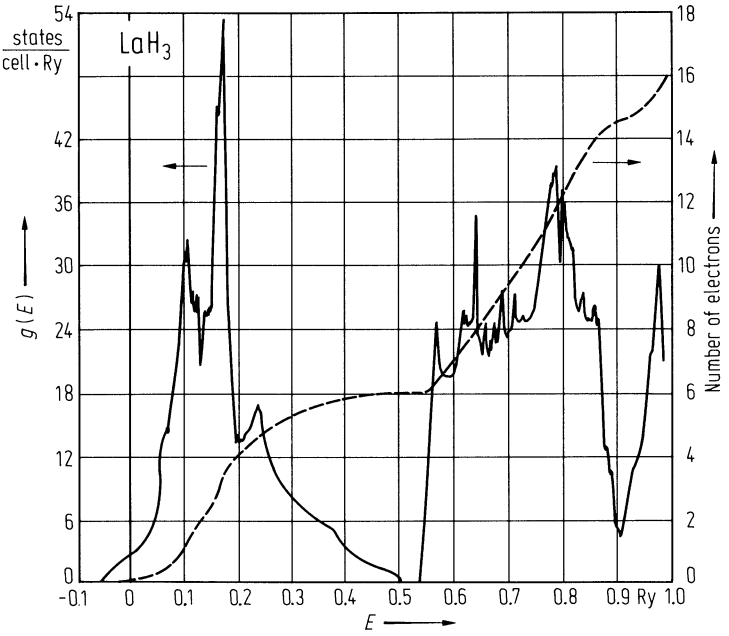

Fig. 12.

LaH_3. Schematic electronic structure of A = La metal, B = up to now used for insulating La compounds, and C = proposed for LaH_3. Arrows indicate core hole screening mechanism [82S]. For a detailed discussion, see original paper.

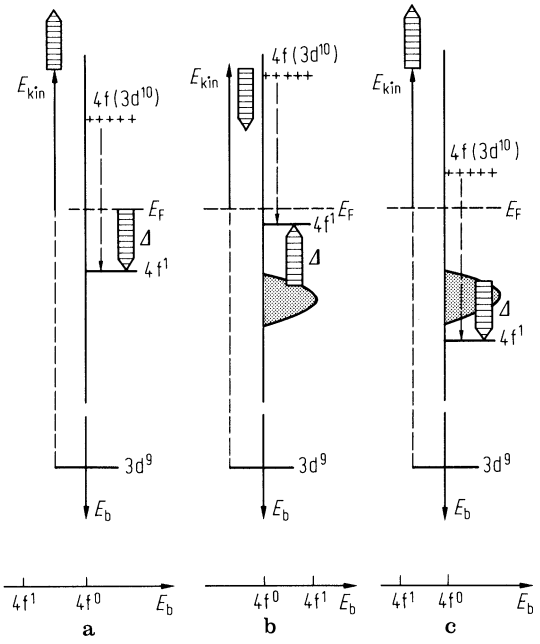

Fig. 13.

$LaH_{2.85}$. Temperature dependence of electrical resistivity [82M]. Inset shows conductivity vs. temperature.

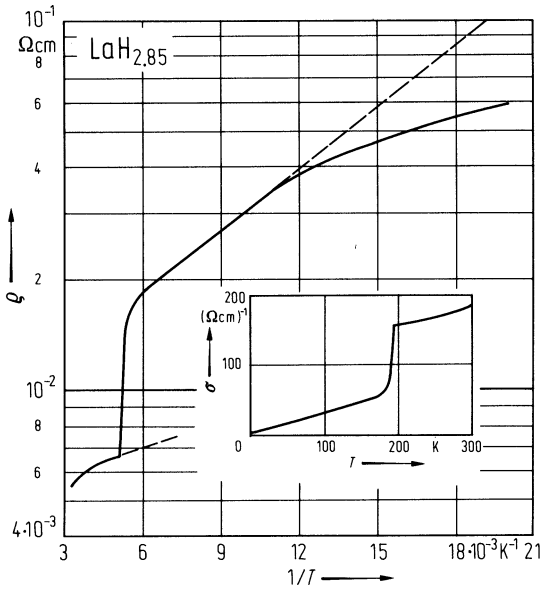

Fig. 14.

LaH_3. XPS valence band and 5p core level spectra (intensity vs. binding energy) [82S].

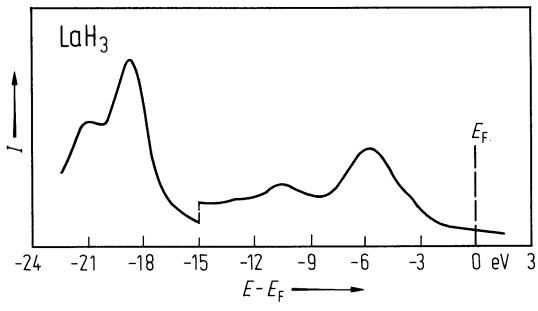

Fig. 15.

LaH_3, La. XPS lanthanum 3d and 1s spectra (intensity vs. binding energy) [82S]. $La(OH)_3$ for comparison.

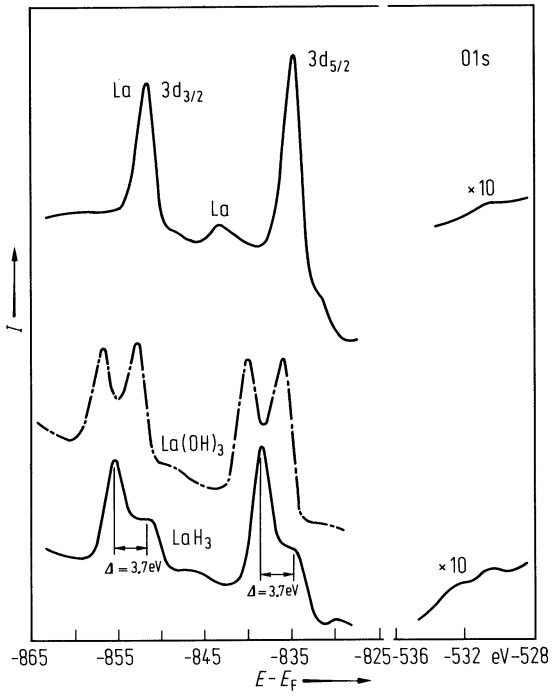

Fig. 16.

$LaH_{2.89}$. Photoelectron energy distribution curves (photoelectron emission intensity vs. initial state energy) showing very weak valence band emission [81P]. Parameter: photon excitation energy.

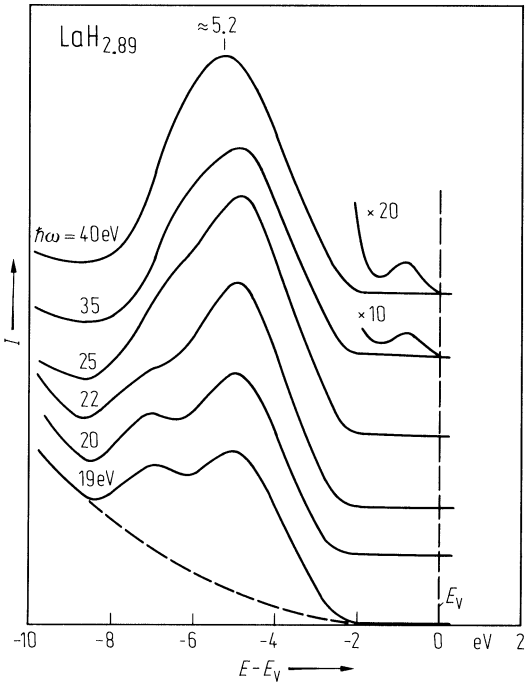

Fig. 17.

$LaH_{2.89}$. Photoelectron energy distribution curves (photoelectron emission intensity vs. initial state energy) for $h\nu$ = 40 eV normalized to the emission from the La 5p core levels [81P].